View metadata, citation and similar papers at core.ac.uk

brought to you by CORE

provided by Universiti Putra Malaysia Institutional Repository

UNIVERSITI PUTRA MALAYSIA

STRUCTURAL ELECTRICAL AND MAGNETIC PROPERTIES OF LA2/3CA1/3MNO3 PEROVSKITES WITH IN, GA AND AL SUBSTITUTION AT EITHER LA OR CA SITE

ABDULLAH CHIK.

FSAS 2004 32

STRUCTURAL, ELECTRICAL AND MAGNETIC PROPERTIES OF $La_{2/3}Ca_{1/3}MnO_3$ PEROVSKITES WITH In, Ga and Al SUBSTITUTION AT EITHER La OR Ca SITE

By

ABDULLAH CHIK

Thesis Submitted to the School of Graduate Studies, Universiti Putra Malaysia, in Fulfilment of the Requirements for the Degree of Doctor of Philosophy

March 2004

UPM

DEDICATIONS

Prof. Dr. Abdul Halim Shaari,

for guidance...

To Prof. Datuk Dr. Mohd Noh Dalimin,

for patience and understanding...

To my wife, Rojita Abdul Hamid, and my two children,

Ahmad Luqman Afiq and Nurul Farzana Aimi

To my mother and father, Hjh. Che Bee Mohd Arshad

and Hj. Chik Hussain

for their love and support...

To Universiti Malaysia Sabah for this opportunity for study leave,

Universiti Putra Malaysia, friends and ex-coursemates !

Abstract of thesis presented to the Senate of Universiti Putra Malaysia in fulfillment of the requirements for the degree of Doctor of Philosophy

STRUCTURAL, ELECTRICAL AND MAGNETIC PROPERTIES OF $La_{2/3}Ca_{1/3}MnO_3$ PEROVSKITES WITH In, Ga and Al SUBSTITUTION AT EITHER La OR Ca SITE

By

ABDULLAH CHIK

March 2004

Chairman : Professor Abdul Halim bin Shaari, Ph.D.

Faculty : Science and Environmental Studies

The structure, electrical and magnetic properties of colossal magnetoresistance material $La_{2/3}Ca_{1/3}MnO_3$ (LCMO) substituted with In, Ga and Al at both La and Ca site have been studied. Samples of $(La_{1-x}In_x)_{2/3}Ca_{1/3}MnO_3$ (LICMO), $(La_{1-x}Ga_x)_{2/3}Ca_{1/3}MnO_3$ (LGCMO), $(La_{1-x}Al_x)_{2/3}Ca_{1/3}MnO_3$ (LACMO), $La_{2/3}(Ca_{1-x}In_x)_{1/3}MnO_3$ (LCIMO), $La_{2/3}(Ca_{1-x}Ga_x)_{1/3}MnO_3$ (LCGMO), $La_{2/3}(Ca_{1-x}Al_x)_{1/3}MnO_3$ (LCAMO) with x=0.0 to 1.0 were prepared using solid state reaction method. X-ray diffraction (XRD) patterns shows single phase pattern at low concentration with increasing intensity of secondary phases at high concentration of dopant. All samples except sample LICMO x=0.6, exhibit orthorhombic structure. Sample LICMO x=0.6 exhibits tetragonal structure. The AC susceptibility studies indicates LICMO, LGCMO, LACMO exhibit wide variety of magnetic phases. For LICMO, LACMO and LGCMO system, ferromagnetic to paramagnetic transition are observed from the undoped sample x=0.0 to 0.5, 0.4 and 0.3 respectively. With further doping at La site, spin glass transition is observed followed by antiferromagnetic to paramagnetic transition with increasing dopant concentration. The Curie temperature, T_C decreases as indium, gallium and aluminum doping increases indicates weakening of

ferromagnetic interactions, but the antiferromagnetic interactions is getting stronger with increasing dopant, resulting spin glass system and antiferromagnetism with further doping concentration. With In, Ga and Al substitution at the Ca site, all samples with the exception of LCIMO x=1.0, exhibit ferromagnetic to paramagnetic transition. For LCIMO sample x=1.0, AC susceptibility study indicates antiferromagnetic to paramagnetic transition. The electrical properties show the metal to insulator transition and this property is limited to certain doping level for both La and Ca site substitution, i.e. until x=0.9 for LICMO, x=0.8 for LGCMO, LACMO, LCIMO and LCGMO, and x=0.5 for LCAMO system. Beyond the specific doping level, the samples become insulator for La site substitution, and semiconducting behaviour for Ca site substitution. This phenomenon is due to the ionic size of dopant for La site substitution, and both ionic size of dopant and decreasing Mn^{4+}/Mn^{3+} ratio due to decreasing Ca^{2+} ions. Fitting of adiabatic small polaron hopping model to high temperature ln(R/T), indicates the activation energies of all samples within range of 0.03eV to 0.17eV which is consistent with reported values in the literature, confirming small polaron hopping activities beyond T_P. Magnetoresistance measurements show that magnetoresistance (MR) ratio is maximum at temperature close to T_P for all samples, and increases with increasing dopant concentration for La site substitution. However, for Ca site substitution, the magnetoresistance's maximum is not as high as La site substitution, and decreases with increasing dopant concentration for $x > 0.3$, because of the low Mn^{4+}/Mn^{3+} ratio that weakened the Zener double exchange interactions and thus the metallic conductivity and ferromagnetism. High MR values are 80% for LICMO sample x=0.4, 95% for LGCMO sample x=0.6 and 87% for LACMO sample x=0.2, compares to 40% of LCMO sample. The Scanning Electron Microscopy (SEM) micrographs indicate

fused and denser grains for all samples. Large abnormal growth is seen only in LICMO for x=0.1 and 0.2 samples and increasing level of porosity with increasing dopant is seen for LACMO, LCGMO and LCIMO samples. LICMO and LGCMO samples exhibit decreasing level of porosity with increasing substitution while LCAMO system has low level of porosity in all samples.

Abstrak tesis yang dikemukakan kepada Senat Universiti Putra Malaysia sebagai memenuhi keperluan untuk ijazah Doktor Falsafah

PENCIRIAN STRUKTUR, ELEKTRIK DAN MAGNET BAGI BAHAN PEROVSKIT $La_{2/3}Ca_{1/3}MnO_3$ DENGAN PENGGANTIAN In, Ga dan Al PADA TAPAK La ATAU Ca

Oleh

ABDULLAH CHIK

Mac 2004

Pengerusi : Profesor Abdul Halim bin Shaari, Ph.D.

Fakulti : Sains dan Pengajian Alam Sekitar

Ciri-ciri struktur, elektrik and magnet bahan bermagnetorintangan kolosal $La_{2/3}Ca_{1/3}MnO_3$ (LCMO), digantikan dengan In, Ga dan Al pada kedua-dua tapak La dan Ca, telah dikaji. Sampel-sampel $(La_{1-x}In_x)_{2/3}Ca_{1/3}MnO_3$ (LICMO), $(La_{1-x}Ga_x)_{2/3}Ca_{1/3}MnO_3$ (LGCMO), $(La_{1-x}Al_x)_{2/3}Ca_{1/3}MnO_3$ (LACMO), $La_{2/3}(Ca_{1-x}In_x)_{1/3}MnO_3$ (LCIMO), $La_{2/3}(Ca_{1-x}Ga_x)_{1/3}MnO_3$ (LCGMO), $La_{2/3}(Ca_{1-x}Al_x)_{1/3}MnO_3$ (LCAMO) dengan x=0.0 ke 1.0 telah disediakan dengan menggunakan kaedah tindakbalas keadaan pepejal. Corak belauan sinar X menunjukkan fasa tunggal pada kepekatan rendah dengan pertambahan keamatan fasa kedua pada kepekatan pendopan yang tinggi. Kesemua sampel-sampel kecuali sampel LICMO x=0.6 mempamerkan struktur ortorombik. Sampel LICMO x=0.6 mempamerkan struktur tetragonal. Kajian kerentanan AC menunjukkan LICMO, LGCMO dan LACMO memperlihatkan pelbagai jenis fasa magnet. Bagi sistem LICMO, LACMO dan LGCMO, peralihan ferromagnet kepada paramagnet masing-masing dicerap daripada sampel x=0.0 ke 0.5, x=0.0 ke 0.4 dan x=0.0 ke 0.3. Dengan pertambahan pendopan di tapak La, peralihan kepada kaca spin dicerap dan diikuti dengan peralihan antiferomagnet kepada paramagnet dengan penambahan kepekatan pendopan. Suhu

Curie, T_C mengurang dengan pertambahan pendopan indium, gallium dan aluminum menunjukkan interaksi ferromagnet yang semakin lemah, dan interaksi antiferromagnet yang semakin kuat, lalu melahirkan sistem spin kaca dan antiferromagnet dengan pertambahan kepekatan pendopan. Dengan penggantian In, Ga dan Al pada tapak Ca, kesemua sampel kecuali LCIMO x=1.0, menunjukkan peralihan ferromagnet kepada paramagnet. Interaksi ferromagnet masih berlaku dengan pertambahan kepekatan pendopan Al dan Ga walaupun pada kepekatan x=1.0. Untuk sampel LCIMO x=1.0, kajian kerentanan AC menunjukkan peralihan antiferromagnet kepada paramagnet. Ciri-ciri elektrik menunjukkan peralihan logam kepada penebat dan ciri ini terhad kepada paras pengdopan tertentu bagi kedua-dua penggantian tapak La dan Ca, contohnya, sehingga x=0.9 untuk LICMO, x=0.8 untuk LGCMO, LACMO, LCIMO dan LCGMO, dan x=0.5 untuk sistem LCAMO. Selepas paras pengdopan tersebut, sampel menjadi penebat bagi penggantian tapak La, dan bagi penggantian tapak Ca, sampel-sampel mempamerkan hanya perlakuan semikonduktor. Fenomena ini disebabkan oleh saiz ion pendopan bagi penggantian tapak La, dan kedua-dua saiz ion pendopan dan pengurangan nisbah Mn^{4+}/Mn^{3+} disebabkan oleh pengurangan ion-ion Ca^{2+}. Lekapan model lompatan polaron kecil adiabatik kepada ln(R/T) pada suhu tinggi, menunjukkan tenaga pengujaan kesemua sampel adalah dalam lingkungan 0.03 eV ke 0.17 eV yang konsisten dengan nilai-nilai dilaporkan dalam literatur, mengesahkan aktiviti lompatan polaron kecil pada suhu melebihi T_P. Penyukatan magnetorintangan menunjukkan nisbah magnetorintangan (MR) adalah maksimum pada suhu menghampiri T_P pada semua sampel, dan bertambah dengan pertambahan kepekatan pendopan pada penggantian tapak La. Walaubagaimanapun, bagi penggantian tapak Ca, megnetorintangan maksima adalah tidak setinggi penggantian pada tapak La, dan berkekurangan

dengan petambahan kepekatan pendopan x > 0.3, kerana nisbah Mn^{4+}/Mn^{3+} yang rendah melemahkan interaksi pertukaran ganda dua Zener dan seterusnya konduksi logam dan feromagnet. Nilai MR yang tinggi adalah 80% bagi sampel LICMO x=0.4, 95% bagi sampel LGCMO x=0.6 dan 87% bagi sampel LACMO x=0.2, berbandingkan 40% sampel LCMO. Mikrograf Mikroskop Elektron Imbasan (SEM) menunjukkan butir-butir tercantum dan lebih tumpat untuk kesemua sampel. Pertumbuhan abnormal yang besar kelihatan hanya pada sampel LICMO x=0.1 dan 0.2 dan pertambahan paras poros dengan pertambahan pendopan dilihat pada sampel-sampel LACMO, LCGMO dan LCIMO. Sampel-sampel LICMO dan LGCMO mempamerkan penurunan paras poros dengan pertambahan penggantian manakala sistem LCAMO mempunyai paras poros yang rendah bagi semua sampel.

ACKNOWLEDGEMENTS

I would like to express my utmost gratitude and appreciation to my project supervisor, Professor Dr. Abdul Halim Shaari for his patience, supervision, guidance, and discussions. I am also very grateful to my co-supervisor, Professor Dr. Wan Mahmood Mat Yunus and Professor Dr. Mohd Maarof H.A. Mokhsin for their comments and suggestions throughout the research work.

I am also expressing my gratitude to Universiti Malaysia Sabah for granting study leave and scholarship for Ph. D study. I would like to thank Tan Sri Professor Datuk Seri Panglima Dr. Abu Hassan Othman for allowing me to complete my work at Universiti Putra Malaysia. I am also grateful to Professor Datuk Dr. Mohd Noh Dalimin for his guidance and suggestions throughout my study leave.

Sincere thanks to Dr. Lim Kean Pah, Dr. Imad Hamadneh, Mrs Iftetan, Ms. Zohra Gebrel, Mr. K.K.Kabashi, Mrs Sharmiwati and Mr Azman Awang Teh for their assistance in samples preparation method, in using resistivity machine, AC susceptometer, magnetoresistance measurements, X ray diffractometer, furnaces and fruitful discussions. I would like also to thank Mr. Razak Harun for all technical favors.

I wish to thank all staffs of Electron Microscope Unit, Faculty of Bioscience, UPM especially Mr. Raffi, Ms. Aini, and Mrs. Faridah for helping me in operating SEM and taking SEM micrographs.

At last but not least, to my loving wife, Rojita Abdul Hamid, for her understanding, caring and continuous support, and my two darling children, Ahmad Luqman Afiq and Nurul Farzana Aimi of whom I cannot live without.

I certify that an Examination Committee met on 29th March 2004 to conduct the final examination of Abdullah Chik on his Doctor of Philosophy thesis entitled "Structural, Electrical and Magnetic Properties of $La_{2/3}Ca_{1/3}MnO_3$ Perovskites with In, Ga and Al Substitution at Either La or Ca Site" in accordance with Universiti Pertanian Malaysia (Higher Degree) Act 1980 and Universiti Pertanian Malaysia (Higher Degree) Regulations 1981. The Committee recommends that the candidate be awarded the relevant degree. Members of the Examination Committee are as follows:

Zainal Abidin Talib, Ph.D.
Associate Professor
Faculty of Science and Environmental Studies
Universiti Putra Malaysia
(Chairman)

Hishamuddin Zainuddin, Ph.D.
Associate Professor
Faculty of Science and Environmental Studies
Universiti Putra Malaysia
(Member)

Elias Saion, Ph.D.
Associate Professor
Faculty of Science and Environmental Studies
Universiti Putra Malaysia
(Member)

Muhammad Yahya, Ph.D.
Director
Center of Academic Advancement
Universiti Kebangsaan Malaysia
(Independent Examiner)

GULAM RUSUL RAHMAT ALI, Ph.D.
Professor/Deputy Dean
School of Graduate Studies
Universiti Putra Malaysia

Date: 17 JUN 2004

This thesis was submitted to the Senate of Universiti Putra Malaysia and has been accepted as partial fulfilment of the requirements for the degree of Doctor of Philosophy. The members of the Supervisory Committee are as follows:

Abdul Halim Shaari, Ph.D.
Associate Professor
Faculty of Science and Environmental Studies
Universiti Putra Malaysia
(Chairman)

Hishamuddin Zainuddin, Ph.D.
Associate Professor
Faculty of Science and Environmental Studies
Universiti Putra Malaysia
(Member)

Elias Saion, Ph.D.
Associate Professor
Faculty of Science and Environmental Studies
Universiti Putra Malaysia
(Member)

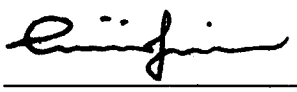

AINI IDERIS, Ph.D.
Professor/Dean
School of Graduate Studies
Universiti Putra Malaysia

Date: 20 JUL 2004

DECLARATION

I hereby declare that the thesis is based on my original work except for quotations and citations which have been duly acknowledged. I also declare that it has not been previously or currently submitted for any other degree at UPM or other institutions.

ABDULLAH CHIK

Date : 07 JUL 2004

TABLE OF CONTENTS

		Page
DEDICATION		ii
ABSTRACT		iii
ABSTRAK		vi
ACKNOWLEDGEMENTS		ix
APPROVAL		xi
DECLARATION		xii
LIST OF TABLES		xvii
LIST OF FIGURES		xix
LIST OF PLATES		xxvii
LIST OF ABREVIATIONS / NOTATIONS / GLOSSARY OF TERMS		xxviii
CHAPTER		
1	**INTRODUCTION**	
	1.1 Colossal Magnetoresistance Phenomenon	1
	1.2 The Need for CMR Material Research	2
	1.3 Application of Manganites	2
	1.4 Objective of the Thesis	4
2	**LITERATURE REVIEW**	
	2.1 Mixed Valence Manganites	7
	2.2 Basic Properties	8
	2.2.1 Crystalline Structure	9
	2.2.2 Electronic Structure	11
	2.2.3 Magnetic Properties	15
	2.2.3.1 Phase Diagram of $La_{1-x}Ca_xMnO_3$	15
	2.3 Colossal Magnetoresistance Phenomenon	17
	2.4 Transport Properties of Manganites	19
	2.4.1 High Temperature Resistivity	20
	2.4.2 Low Temperature Resistivity	20
	2.5 Lattice Effect	21
3	**THEORETICAL MODELS FOR CMR**	
	3.1 Introduction	25
	3.2 Magnetic Interaction	25
	3.2.1 Super Exchange	26
	3.2.2 Double Exchange	26
	3.2.3 Semicovalence Exchange	28
	3.3 Charge Carriers Localizations	30
	3.3.1 Self Trapping of Carriers	30
	3.3.2 Charge Transport at Higher Temperatures	32
	3.3.3 Disorder Induced Localizations	33
4	**SAMPLE PREPARATION AND CHARACTERIZATION**	
	4.1 Samples Preparation	35

4.1.1 Chemical Powder Weighing 35
4.1.2 Chemical Mixing 37
4.1.3 Calcination 37
4.1.4 Grinding and Compacting 39
4.1.5 Sintering 39
4.2 Sample Characterisations 40
4.2.1 X ray Diffratometer 40
4.2.2 Four Point Probe 42
4.2.3 AC Susceptometer 42
4.2.4 Scanning Electron Microscope 44
4.2.5 Magnetoresistance Measurement 45

5 RESULTS AND DISCUSSION
5.1 Introduction 46
5.2 Effect of In, Ga and Al substitution for La site in $La_{2/3}Ca_{1.3}MnO_3$ 47
5.2.1 LICMO System
Structural properties 47
Magnetic properties 49
AC susceptibility analysis of LICMO samples 49
Curie Weiss law analysis of LICMO samples 53
Curie Temperature, T_C, of LICMO samples 58
Electrical properties 60
Resistance and phase transition temperature, T_P 60
The dR/dT analysis of LICMO samples 65
Activation energy of LICMO samples 68
Microstructure properties 71
Magnetoresistance properties of LICMO samples 74
Phase diagram for LICMO system 79
5.2.2 LGCMO System
Structural properties 81
Magnetic properties 83
AC susceptibility analysis of LGCMO samples 83
Curie Weiss law analysis of LGCMO samples 86
Curie Temperature, T_C, of LGCMO samples 89
Electrical Properties 91
Resistance and phase transition temperature, T_P 91
The dR/dT analysis of LGCMO samples 96
Activation energy of LGCMO samples 99
Microstructure properties 102
Magnetoresistance properties of LGCMO samples 105
Phase diagram for LGCMO system 110
5.2.3 LACMO System
Structural Properties 112
Magnetic Properties 114
AC susceptibility analysis of LACMO samples 114
Curie Weiss law analysis of LACMO samples 117
Curie Temperature, T_C, of LACMO samples 122
Electrical Properties 123
Resistance and phase transition temperature, T_P 123

The dR/dT analysis of LACMO samples 128
Activation energy of LACMO samples 132
Microstructure properties 134
Magnetoresistance properties of LACMO samples 137
Phase diagram for LACMO system 142
5.3 Effect of In, Ga and Al substitution for Ca site in $La_{2/3}Ca_{1.3}MnO_3$ 143
5.3.1 LCIMO System
Structural properties 143
Magnetic properties 145
AC susceptibility analysis of LCIMO samples 145
Curie Weiss Law analysis of LCIMO samples 148
Curie Temperature, T_C, of LCIMO samples 152
Electrical properties 154
Resistance and phase transition temperature, T_P 154
The dR/dT analysis of LCIMO samples 158
Activation energy of LCIMO samples 161
Microstructure properties 163
Magnetoresistance properties of LCIMO samples 167
Phase diagram for LCIMO system 172
5.3.2 LCGMO System
Structural properties 173
Magnetic properties 175
AC susceptibility analysis of LCGMO samples 175
Curie Weiss law analysis of LCGMO samples 178
Curie temperature, T_C, of LCGMO samples 181
Electrical properties 183
Resistance and phase transition temperature, T_P 183
The dR/dT analysis of LCGMO samples 187
Activation energy of LCGMO samples 190
Microstructure properties 192
Magnetoresistance properties of LCGMO samples 196
Phase diagram of LCGMO system 201
5.3.3 LCAMO System
Structural properties 203
Magnetic properties 205
AC susceptibility analysis of LCAMO samples 205
Curie Weiss Law analysis of LCAMO samples 208
Curie Temperature, T_C, of LCAMO samples 212
Electrical properties 214
Resistance and phase transition temperature, T_P 214
The dR/dT analysis of LCAMO samples 217
Activation energy of LCAMO samples 220
Microstructure properties 222
Magnetoresistance properties of LCAMO samples 226
Phase diagram for LCAMO system 231

6 COMPARISON AMONG SIX SYSTEMS
6.1 Comparison among La site substitution samples 232
6.1.1 The phase transition temperature, T_P 232

6.1.2 The magnetic transition temperature, T_M 233
6.2 Comparison among Ca site substitution samples 235
6.2.1 The phase transition temperature, T_P 235
6.2.2 The magnetic transition temperature, T_M 236
6.3 Comparison between substitution in La Site and Ca Site 238
6.3.1 The phase transition temperature, T_P 238
6.3.2 The magnetic transition temperature, T_M 241
6.4 Discussion 244

7 CONCLUSIONS AND SUGGESTIONS
7.1 Conclusions 246
7.2 Suggestions for future research 251

REFERENCES/BIBLIOGRAPHY 252
APPENDICES 257
BIODATA OF THE AUTHOR 262

LIST OF TABLES

Tables		Page
5.1	The lattice parameters for LICMO samples x=0.0 to 1.0.	48
5.2	The magnetic transition temperature and the paramagnetic Curie temperature for LICMO samples x=0.0 to x=0.7.	58
5.3	Phase transition temperature for LICMO system.	65
5.4	Activation energies of LICMO samples by fitting using adiabatic small polaron and thermally activated models.	70
5.5	The lattice parameters for LGCMO samples.	82
5.6	The magnetic transition temperature and the paramagnetic Curie temperature for LGCMO samples x=0.0 to x=0.7.	90
5.7	Phase transition temperature for LGCMO system.	95
5.8	Activation energies of LGCMO samples by fitting using adiabatic small polaron.	101
5.9	The lattice parameters for LACMO samples.	112
5.10	The magnetic transition temperature for LACMO samples x=0.0 to x=0.9.	122
5.11	Phase transition temperature for LACMO system.	127
5.12	Activation energies of LACMO samples by fitting using adiabatic small polaron models.	133
5.13	The lattice parameters for LCIMO samples.	143
5.14	The magnetic transition temperature and the paramagnetic Curie temperature for LCIMO samples x=0.0 to x=1.0.	153
5.15	Phase transition temperature for LCIMO system.	157
5.16	Activation energies of LCIMO samples by fitting using adiabatic small polaron models.	163
5.17	The lattice parameters for LCGMO samples.	174
5.18	The magnetic transition temperature for LCGMO samples x=0.0 to x=0.9.	183
5.19	Phase transition temperature for LCGMO system.	186

5.20	Activation energies of LGCMO samples by fitting using adiabatic small polaron models.	192
5.21	The lattice parameters for LCAMO samples.	204
5.22	The magnetic transition temperature for LACMO samples x=0.0 to x=0.9.	213
5.23	Phase transition temperature for LCAMO system.	217
5.24	Activation energies of LCAMO samples by fitting using adiabatic small polaron models.	221
A.1	Apparatus uncertainties for this PhD's project.	257
B.1	The uncertainties of quantities measured in this PhD's project.	261

LIST OF FIGURES

Figures		Page
2.1	The ideal perovskite structure is cubic $T_{1-x}D_xMnO_3$	10
2.2	(a) The O type orthorhombic $GdFeO_3$ structure. This is the distorted version of the ideal cubic perovskite structure with a buckling of the oxygen octahedral to accommodate smaller A cation. (b) The O' type orthorhombic $LaMnO_3$ structure with a Jahn Teller distortion of the oxygen octahedral.	11
2.3	The splitting of crystal field of the five fold degenerate 3d levels in a Mn^{3+} atom.	13
2.4	The schematic illustration of orbital overlap in the perovskite structure.	14
2.5	Jahn Teller distortion lifting the degeneracy of the 3d orbitals in Mn^{3+}.	14
2.6	Phases diagram for $La_{1-x}Ca_xMnO_3$. The states shown are antiferromagnetic insulator (AFI), ferromagnetic insulator (FI), ferromagnetic metallic (FM), charge ordered insulating (COI), and antiferromagnetic insulator (AFI).	16
2.7	(a)Types of antiferromagnetic order in the perovskite structure (b) Spin, charge, and orbital ordering pattern of the CE type observed for manganites with doping level x=1/2.	16
2.8	The temperature dependence of resistivity of $La_{2/3}(Pb,Ca)_{1/3}MnO_3$ single crystals at various applied magnetic field. Inset shows magnetization in the transition region.	17
2.9	Phase diagram of temperature versus tolerance factor for $T_{0.7}D_{0.3}MnO_3$ where T is a trivalent ion and D is a divalent ion.	21
3.1	Examples of superexchange mechanisms in manganites.	26
3.2	Double exchange mechanism involving simultaneous transfer of electron from Mn^{3+} to O^{2-} and from O^{2-} to Mn^{4+}.	28
3.3	Semicovalence mechanism involving (a) antiferromagnetic, (b) ferromagnetic interactions between two neighboring Mn ions.	29

3.4	A small polaron formed by an electron self trapped by the equilibrium atomic displacement pattern around it.	31
3.5	One-dimensional picture of both magnetic and non magnetic disorder in manganites including Coulomb potential variation (solid line).	34
4.1	Schematics of solid state reaction method for preparing ceramic samples.	36
4.2	Schematic representation of calcinations stage.	38
4.3	Schematic representation of sintering stage.	40
4.4	Schematic representation of magnetoresistance measurement.	46
5.1	The x ray diffractogram for LICMO systems.	47
5.2	The cell volume of LICMO system.	49
5.3	Thermal variation of normalized ac susceptibility for LICMO samples (a) for samples x=0.0 to 0.9, (b) x=0.0 to 0.3, (c) x=0.4 to 0.6 (d) x=0.5, (e) x=0.6 to 0.9.	53
5.4	The inverse of magnetic susceptibility versus temperature for selected (a) x=0.0 to 0.9, (b) x=0.0 to 0.3, (c) x=0.4 to 0.6 (d) x=0.7 to 0.9.	56
5.5	The deviation from the Curie Weiss expression for LICMO samples x=0.0 to x=0.5.	57
5.6	The magnetic transition temperature of LICMO samples.	59
5.7	The temperature dependent normalized resistance of LICMO samples (a) x=0.0 to 0.9, (b) x=0.0 to 0.2, (c) x=0.3 to 0.5, (d) x=0.6 to 0.7, (e) x=0.8 to 0.9.	62
5.8	The In concentration dependence of T_P for LICMO samples	63
5.9	The dR/dT vs temperature for LICMO systems (a) x=0.0, 0.1, 0.2, (b) x=0.3, x=0.4 x=0.5 (c) x=0.6, x=0.7 (d) x=0.8 to x=0.9	67
5.10	The fitting of LICMO samples using adiabatic small polaron hopping model.	69
5.11	The activation energies of LICMO samples fitted using small polaron hopping.	69

5.12	Sample density of LICMO system.	71
5.13	SEM image of the fracture surface of LICMO system.	73
5.14	The temperature variation of magnetoresistance of LICMO samples for applied field 1.0 Tesla at (a) 100K, (b) 150K, (c) 200K, (d) 250K, (e) 300K, (f) 100 to 300K.	78
5.15	The phase diagram of the LICMO system.	80
5.16	The x ray diffractogram for LGCMO system.	81
5.17	The cell volumes of the LGCMO samples.	82
5.18	Thermal variation of normalized ac susceptibility for LGCMO samples (a) for samples x=0.0 to 0.9, (b) x=0.0 to 0.3 (c) x=0.3 to 0.6 (d) x=0.6 to 0.9.	85
5.19	The inverse of magnetic susceptibility versus temperature for (a) x=0.0 to 0.9 (b) x=0.0 to 0.3, (b) x=0.4 to 0.6, (c) x=0.7 to 0.9.	88
5.20	The deviation from the Curie Weiss expression for LGCMO samples x=0.0 to x=0.5.	89
5.21	The Curie temperature, T_C, the Neel temperature, T_N, freezing temperature, T_f, of LGCMO samples.	90
5.22	The temperature variation normalized resistance of LGCMO samples from (a) x=0.0 to 0.8 (b) x=0.0 to 0.2, (c) x=0.3 to 0.5, (d) x=0.6 to 0.8 (e) x=0.8.	94
5.23	The temperature variation of maximum normalized resistance versus Ga concentration x.	96
5.24	The dR/dT vs temperature for LGCMO systems (a) x=0.0, 0.1, (b) x=0.3, x=0.4, (c) x=0.5 and 0.6, (d) x=0.7, (e) x=0.8	99
5.25	The fitting of LGCMO samples using adiabatic small polaron hopping model.	100
5.26	The activation energies for small polaron hopping for LGCMO samples.	101
5.27	Sample density of LGCMO system.	102
5.28	SEM image of the fracture surface of LGCMO system.	104

5.29	The temperature variation of magnetoresistance of LGCMO samples for applied field 1.0 Tesla.	108
5.30	The phase diagram of the LGCMO system.	111
5.31	The x ray diffractogram for LACMO system.	113
5.32	The evolution of cell volumes of the LACMO samples.	114
5.33	Thermal variation of normalized ac susceptibility for LACMO samples (a) for samples x=0.0 to 0.9, (b) samples x=0.0 to 0.3 (c) samples x=0.4 to 0.6, (d) samples x=0.7 to 0.9.	117
5.34	The inverse of magnetic susceptibility versus temperature for selected LACMO samples (a) x=0.0 to 0.1. (b) x=0.2 to 0.6 (c) x=0.7 to 0.9.	120
5.35	The deviation from the Curie Weiss expression for LACMO samples.	121
5.36	The T_M versus Al concentration x for LACMO samples	123
5.37	The temperature variation normalized resistance of LACMO samples from (a) x=0.0 to 0.8, (b) x=0.0 to 0.1, (c) x=0.2 to 0.4, (d) x=0.5 to 0.6, (e) x=0.7, (f) x=0.8.	126
5.38	The phase transition temperature versus Al concentration x for LACMO system.	128
5.39	The dR/dT vs temperature for LACMO systems (a) x=0.0, 0.1, (b) x=0.2, x=0.3, (c) x=0.4 and 0.5, (d) x=0.6, (e) x=0.7to x=0.8 .	131
5.40	The fitting of LACMO samples using adiabatic small polaron hopping model	132
5.41	The activation energies for small polaron happing for LACMO samples.	133
5.42	Sample density of LACMO system.	134
5.43	SEM image of the fracture surface of LACMO system.	136
5.44	The magnetoresistance of LACMO samples at temperature (a) 100K, (b) 150K, (c) 200K, (d) 250K, (e) 300K, (f) 100K to 300K with applied field 1.0 Tesla.	141
5.45	The phase diagram of the LACMO system.	142

5.46	The x ray diffractogram for LCIMO system.	144
5.47	The evolution of cell volumes of the LCIMO samples.	144
5.48	Thermal variation of normalized ac susceptibility for LCIMO samples (a) for samples x=0.0 to 1.0, (b) samples x=0.0 to 0.4 (c) samples x=0.5 to 0.7, (d) samples x=0.8 to 1.0.	147
5.49	The inverse of magnetic susceptibility versus temperature for selected LCIMO samples (a) x=0.0 to 1.0. (b) x=0.0 to 0.3 (c) x=0.4 to 0.6 (d) x=0.7 to 1.0	150
5.50	The deviation from the Curie Weiss expression for LCIMO samples.	151
5.51	The Curie temperature, T_C ,versus In content x for LCIMO samples.	153
5.52	The temperature variation normalized resistance of LCIMO samples from (a) x=0.0 to 1.0, (b) x=0.0 to 0.3, (c) x=0.4 to 0.6, (d) x=0.7 to 1.0.	156
5.53	The phase transition temperature versus In concentration x for LCIMO system.	158
5.54	The dR/dT vs temperature for LCIMO systems (a) x=0.0, 0.2, (b) x=0.3 to x=0.5, (c) x=0.6 to 0.9, (d) x=1.0,	160
5.55	The plot of ln(R/T) vs temperature for LCIMO samples.	162
5.56	The activation energies for small polaron happing for LCIMO samples.	162
5.57	Sample density of LCIMO system.	164
5.58	SEM image of the fracture surface of LCIMO system.	166
5.59	The Applied field variations fo MR% for various temperatures, (a) 100K, (b) 150K, (c) 200K, (d) 250K and (e) 300K.	171
5.60	The temperature variation of magnetoresistance of LCIMO samples for applied field 1.0 Tesla.	171
5.61	The phase diagram of the LCIMO system.	172
5.62	The x ray diffractogram for LCGMO system.	173
5.63	The evolution of cell volumes of the LCGMO samples	175